Carbohydrate Polymers 100 (2014) 116–125

Contents lists available at ScienceDirect

Carbohydrate Polymers

journal homepage: www.elsevier.com/locate/carbpol

Synthesis and structure–property evaluation of cellulose ω-carboxyesters for amorphous solid dispersions

Haoyu Liu[a,b], Grace A. Ilevbare[c], Benjamin P. Cherniawski[a], Earl T. Ritchie[a], Lynne S. Taylor[c], Kevin J. Edgar[a,b,*]

[a] Macromolecules and Interfaces Institute, Virginia Tech, Blacksburg, VA 24061, United States
[b] Department of Sustainable Biomaterials, College of Natural Resources and Environment, Virginia Tech, Blacksburg, VA 24061, United States
[c] Department of Industrial and Physical Pharmacy, College of Pharmacy, Purdue University, West Lafayette, IN 47907, United States

ARTICLE INFO

Article history:
Received 15 August 2012
Received in revised form
14 November 2012
Accepted 18 November 2012
Available online 27 November 2012

Keywords:
Cellulose ω-carboxyalkanoates
Crystal growth inhibition
Amorphous solid dispersion
Oral drug delivery
Cellulose esters
Cellulose acylation

ABSTRACT

The use of amorphous solid dispersions (ASDs) is an effective and increasingly widely used approach for solubility enhancement of drugs and drug candidates with poor aqueous solubility. Successful molecular dispersion of drugs in polymer matrices requires new polymers that are designed to meet all ASD requirements, including drug release and prevention of drug recrystallization in storage or from solution. We describe herein design and synthesis of a new series of cellulose ω-carboxyalkanoates for ASDs, by reaction of cellulose with long-chain diacids that have been monoprotected as benzyl esters at one end, and monoactivated as acid chlorides at the other. Glass transition temperatures (T_g) of these cellulose ω-carboxyesters exceed ambient temperature by at least 50 °C, providing a sufficient ΔT to prevent drug mobility and crystallization. Cellulose acetate suberates and sebacates prepared in this way are extraordinary solution crystal growth inhibitors for the poorly soluble anti-HIV drug ritonavir. These new cellulose ω-carboxyesters have strong potential as ASD polymers for enhancement of drug solubility and bioavailability.

1. Introduction

Cellulose esters have a long history of effective use in pharmaceutical applications, based on their low toxicity, water permeability, essentially complete lack of ability to permeate through the enterocytes into the circulation, and the possibility of tailoring the cellulose ester structure to impart, for example, pH responsiveness (Edgar et al., 2001). More recently, cellulose esters have been explored as key components of advanced drug delivery systems addressing difficult issues like poor drug bioavailability (Friesen et al., 2008) and nanoparticulate therapy (Mawad et al., 2009). Cellulose esters are more useful in oral drug administration than in modes like intravenous or inhalation therapy, since humans lack the ability to metabolize and clear cellulose from the circulation. Oral drug administration is generally preferred by patients, due to its unsurpassed convenience, potential for outpatient therapy, and relatively low cost, but the ability to administer drugs orally is currently limited by physical characteristics of drugs and drug candidates.

Poor drug solubility, and the low bioavailability that often results, is a particular problem in modern oral drug therapy. The process of high throughput screening of drug candidates against often hydrophobic receptor binding sites, with selection based on magnitude of binding constant, leads inevitably to a plethora of hydrophobic drug candidates. The need for purity of drug candidates leads drug developers to favor highly crystalline molecules. These two properties, hydrophobicity and high crystallinity, are inimical to water solubility. As a result, a high proportion of new and existing drugs and drug candidates has poor aqueous solubility (estimated as high as 40–70%) (Hauss, 2007).

In recent years, amorphous solid dispersion has emerged as an effective approach to enhancing drug solubility (Alonzo et al., 2011; Konno, Handa, Alonzo, & Taylor, 2008; Newman, Knipp, & Zografi, 2012). To create an ASD of a particular drug, the drug is dispersed, ideally molecularly, in a polymer matrix. The creation of a miscible drug-polymer blend leads to a high-energy, amorphous state of the drug, where the polymer inhibits drug crystallization. This enhances drug solution concentration by reducing the kinetic energy barrier that must be surmounted for the drug to dissolve. The criteria for the polymer may be summarized as follows:

- Polymer and any decomposition products must be non-toxic.
- Polymer must be miscible with the active drug, and prevent drug crystallization during transport and storage, even in hot,

* Corresponding author at: Department of Sustainable Biomaterials, College of Natural Resources and Environment, Virginia Tech, Blacksburg, VA 24061, United States. Tel.: +1 540 231 0674; fax: +1 540 231 8176.
E-mail address: kjedgar@vt.edu (K.J. Edgar).

0144-8617/$ – see front matter © 2012 Elsevier Ltd. All rights reserved.
http://dx.doi.org/10.1016/j.carbpol.2012.11.049

humid ambient environments, for at least several years (Hancock, Shamblin, & Zografi, 1995).
- Must prevent or severely retard drug crystallization after release but prior to absorption, in aqueous solution (Alonzo, Zhang, Zhou, Gao, & Taylor, 2010; Ilevbare, Liu, Edgar, & Taylor, 2012b).
- Must release the drug effectively in the absorptive zone of the digestive tract (Edgar et al., 2001; Posey-Dowty et al., 2007).

Polymers used for ASD to date have largely been selected from those already in approved pharmaceutical formulations, rather than having been designed for ASD requirements. Some of these polymers can themselves crystallize during storage (poly(ethylene glycol)), so are not suitable from a stability perspective. Poly(vinylpyrrolidinone) (PVP) is an excellent polymer for ASD of drugs, but is highly soluble in water, especially at low (gastric) pH; thus overly fast release or undesired exposure of stomach to drug can be problems. Hydroxypropyl methyl cellulose acetate succinate (HPMCAS) is also quite effective in ASD of drugs. However HPMCAS is complex to synthesize and analyze; amounts of four separate substituents must be controlled, and the hydroxypropyl substituent carries the additional complication that it can form oligomeric poly(hydroxypropyl) side chains of various lengths from the cellulosic hydroxyl initiator. The overall hypothesis in the collaborative ASD work between the Taylor and Edgar groups is that, by understanding the fundamental science and specific performance requirements for ASDs and ASD polymers, we can design, synthesize and use polymers with superior performance in ASD systems that meet all system requirements.

In previous work, we have reported that cellulose esters containing adipate groups have useful combinations of properties as ASD polymers (Kar, Liu, & Edgar, 2011; Liu, Kar, & Edgar, 2012). The tetramethylene side chains of the adipate groups accentuate the already hydrophobic nature of the cellulose esters, enhancing miscibility with hydrophobic drugs and enabling slow drug release. The carboxyl end groups not only provide specific interactions with hydrogen bond acceptors on the drug, enhancing miscibility and stability, but also provide a mechanism for drug release through ionization and subsequent swelling upon reaching the neutral environment of the small intestine. In our previous studies, cellulose acetate adipate propionate (CAAdP) was found to be an effective inhibitor of crystal growth of the important, hydrophobic drug ritonavir at supersaturations lower than that generated during the dissolution of the amorphous form (Ilevbare, Liu, Edgar, & Taylor, 2012a; Ilevbare et al., 2012b); ritonavir is an important metabolic inhibitor that is a key component of several drug formulations used in human immunodeficiency virus (HIV) therapy (Cameron et al., 1999) and is administered as the amorphous form. These structure–property studies showed that both the hydrophobicity of the polymer and its carboxyl group content were important contributors predicting strong inhibition of ritonavir crystallization, and that crystal growth inhibition was highly sensitive to these parameters; indeed, the closely related cellulose acetate adipate butyrate (CAAdB) was ineffective in inhibiting ritonavir crystal growth. In related research in our groups (Li, Konecke, Wegiel, Taylor, & Edgar, 2012), amorphous solid dispersion in CAAdP matrices has been shown not only to strongly inhibit crystallization from either solid dispersion or aqueous solution of the biologically potent but poorly soluble flavonoid curcumin, but remarkably also protected curcumin against the rapid chemical degradation (retro-aldol reaction) that occurs in the absence of polymer.

The hypothesis of the current study is that further exploration of this ASD structure–property relationship, through synthesis of novel cellulose ω-carboxyalkanoates bearing longer, more hydrophobic tethers between the cellulose main chain and the pendent carboxyl group, will lead to even more effective ASD polymers. In this way we hoped both to expand the breadth of our ability to enhance drug solubility and bioavailability by ASD (making it effective for an even broader range of drug structures), and to enhance the stability of the drug in the ASD, permitting longer term stabilization of maximum solution concentrations attainable from amorphous drug (increasing bioavailability). This paper describes the development of methods for the synthesis and characterization of soluble, non-crosslinked cellulose esters containing suberate or sebacate groups, as well as the results of preliminary structure–property investigations that demonstrate the great promise of these new polymers for amorphous solid dispersions of poorly soluble drugs.

2. Experimental

2.1. Materials

Microcrystalline cellulose (MCC, Avicel® PH-101, Fluka) was dried under reduced pressure at 50 °C overnight prior to use. Cellulose acetate propionate (CAP-504-0.2), cellulose acetate butyrate (CAB-553-0.4) and cellulose acetate (CA 320S) were obtained from Eastman Chemical Co. and dried overnight under vacuum at 40 °C prior to use. *N*,*N*-dimethylacetamide (DMAc) and 1,3-dimethyl-2-imidazolidinone (DMI) were purchased from ACROS Organics and dried over 4 Å molecular sieves. Other purchased reagents were used as received. Suberic acid, sebacic acid, methyl ethyl ketone (MEK), *p*-toluenesulfonic acid (PTSA), triethylamine (Et_3N), oxalyl chloride and anhydrous tetrahydrofuran were purchased from ACROS Organics. Toluene, benzyl alcohol, *N*,*N*-dimethylformamide (DMF), dichloromethane, lithium chloride and sodium bicarbonate were purchased from Fisher Scientific. Hydrogenolysis catalyst 20% Pd(OH)/C was obtained from Sigma–Aldrich. Ritonavir was purchased from Attix Corporation, Toronto, Ontario, Canada.

2.2. Measurements

^{1}H NMR spectra were acquired on INOVA 400 or Bruker Avance 500 spectrometers. Samples were analyzed as solutions in $CDCl_3$ or DMSO-d_6 (ca. 10 mg/mL) at 25 °C in standard 5 mm o.d. tubes. A drop of trifluoroacetic acid was added to shift the water peak of DMSO-d_6 downfield from the spectral region of interest. 32 scans were obtained for each sample. ^{13}C NMR spectra were obtained on a Bruker Avance 500 MHz spectrometer with a minimum of 5000 scans in DMSO-d_6 (ca. 50 mg/mL) at 80 °C. DSC analyses of cellulosic polymers were performed on a TA Instruments Q2000 apparatus. Dry powders (ca. 5 mg) were loaded in Tzero™ aluminum pans. Each sample was equilibrated at 30 °C and then heated to 180 °C at 15 °C/min. The sample then was cooled at 50 °C/min to −50 °C. During the second heating cycle the sample was heated to 180 °C at 15 °C/min. All DSC measurements were verified with a duplicate run. T_g values were recorded as the step-change inflection point from 2nd heat scans. IR spectra were obtained on a Nicolet 8700 instrument. Size exclusion chromatography (SEC) was performed in HPLC grade THF at 40 °C at flow rate 1 mL/min using a Waters size exclusion chromatograph equipped with an autosampler, three in-line 5 μm PLgel Mixed-C columns, and a Waters 410 refractive index (RI) detector operating at 880 nm, which was programmed to a polystyrene calibration curve. We report number average molecular weights relative to polystyrene standards. Cellulose ester solubility was tested by adding ca. 10 mg of sample into 2 mL each of various solvents. Each mixture was subjected to vortex mixing for 5–10 min at room temperature, then solubility was judged by visual examination.

Thermal analysis of the solid dispersion was carried out through the use of a modulated differential scanning calorimeter (Model Q2000, TA Instruments). The calorimeter was calibrated with sapphire and indium standards under N_2. For each measurement a

sample of approximately 2–5 mg was heated to 180 °C at 20 °C/min to remove moisture. Then the sample was cooled to −78 °C at 50 °C/min, followed by the second heating scan to 180 °C at 20 °C/min. From this second scan the T_g was measured and the lack of crystallization or melting transitions was confirmed. DSC heating curves were analyzed using Universal Analysis 2000 software (TA instruments). Powder X-ray diffraction (PXRD) data were collected using a Bruker D8 Discover X-ray Diffractometer. Cu Kα (λ = 0.154 nm) radiation was at 40 kV/40 mA and the diffraction profile was detected using a locked couple 2 theta scan from 10 to 50° scattering angle. The scan speed was 0.1 s/step with the increment of 0.01°. XRD samples were prepared by flattening the lyophilized solid dispersions into powder form onto a glass slide.

2.3. Methods

Synthesis of monobenzyl sebacate (Supplementary material, Scheme S1). The method of English, Girard, Jasys, Martingano, and Kellogg (1990) was adapted for the synthesis of monobenzyl sebacate. Sebacic acid (0.25 mol, 50.56 g), toluene (200 mL), benzyl alcohol (0.30 mol, 1.2 equiv., 32.4 g, 31.1 mL), and *p*-toluene sulfonic acid (2.5 mmol, 0.475 g) were combined in a Dean–Stark apparatus and refluxed until the desired volume of H_2O (0.30 mol, 5.40 mL) was collected from the Fischer esterification of the sebacic acid, indicating the end of the reaction. The mixture was allowed to cool to room temperature, then 150 mL of DI water was added to the reaction. Using vigorous mixing, this mixture was adjusted to pH 9 with 6 M NaOH. The aqueous layer with the di-acid and mono-ester was separated and washed twice with 50 mL of diethyl ether; these diethyl ether washes contained primarily the dibenzyl ester by-product, and were discarded. Diethyl ether (200 mL) was combined with the aqueous layer which was acidified to pH of 2.0–2.5 with 6 M HCl. The ether layer containing the mono-ester was separated. To purify further, the ether layer was washed with 1 M $NaHCO_3$. The ether layer then was concentrated under reduced pressure and vacuum-dried for 1.5 h to yield the final product as white, needle-like solid. Yield: 29.0% (16.96 g, 0.058 mol). ^{1}H NMR ($CDCl_3$): 1.29 (m, 8H), 1.62 (m, 4H), 2.33 (m, 4H), 5.11 (s, 2H), 7.35 (m, 5H).

A similar procedure was followed to synthesize monobenzyl suberate (colorless oil). Yield: 47.5% (31.35 g, 0.12 mol). ^{1}H NMR ($CDCl_3$): 1.33 (m, 4H), 1.63 (m, 4H), 2.33 (m, 4H), 5.11 (s, 2H), 7.34 (m, 5H).

Synthesis of monobenzyl sebacoyl chloride (Supplementary material, Scheme S1). The procedure was adapted from Abell, Morris, and Litten (1990), as follows. Monobenzyl sebacate (0.051 mol, 15.00 g) was dissolved in dichloromethane (300 mL), then DMF (5 drops) was added. The solution was cooled in an ice bath to 0 °C. Oxalyl chloride (24.42 mL, 5.6 equiv.) was added slowly. The ice bath was removed and the reaction proceeded at room temperature. A halt in gas evolution indicated completion, then solvent was removed under reduced pressure. Toluene (50 mL) was added and the product concentrated azeotropically under reduced pressure. The product was stored and used in this crude form without further purification. Yield: 90.1% (0.046 mol, 14.35 g). ^{1}H NMR ($CDCl_3$): 1.30 (m, 8H), 1.67 (m, 4H), 2.35 (t, 2H), 2.86 (t, 2H), 5.11 (s, 2H), 7.35 (m, 5H).

A similar procedure was followed to synthesize monobenzyl suberoyl chloride. Yield: 90.7% (0.051 mol, 14.54 g). ^{1}H NMR ($CDCl_3$): 1.34 (m, 4H), 1.66 (m, 4H), 2.36 (t, 2H), 2.86 (t, 2H), 5.12 (s, 2H), 7.35 (m, 5H).

Preparation of benzyl cellulose acetate propionate suberate/sebacate (Scheme 1). CAP-504-0.2 (1.00 g, 3.56 mmol) was dissolved in MEK (20 mL), and the solution was heated to 60 °C with stirring under nitrogen. Triethylamine (0.54 mL, 3.92 mmol, 1.1 equiv.) was added to the solution. Monobenzyl sebacoyl chloride (1.11 g, 3.56 mmol, 1 equiv.) or monobenzyl suberoyl chloride (1.02 g, 3.56 mmol, 1 equiv.) was added dropwise and allowed to react at 60 °C for 20 h. The reaction mixture was diluted with ∼10 mL of acetone and filtered to remove in situ formed triethylamine hydrochloride precipitate. The remaining solution was precipitated into water (250 mL). The precipitate was collected and washed with isopropanol. The filtered product was redissolved in a minimal amount of chloroform and reprecipitated in hexanes.

Benzyl CAP sebacate yield. 89.1% (3.17 mmol, 1.10 g). ^{1}H NMR ($CDCl_3$): 0.95–1.20 ($COCH_2CH_3$ of propionate), 1.30 ($COCH_2CH_2CH_2CH_2CH_2CH_2CH_2CH_2CO$ of sebacate), 1.63 ($COCH_2CH_2CH_2CH_2CH_2CH_2CH_2CH_2CO$ of sebacate), 2.13–2.44 ($COCH_2CH_2CH_2CH_2CH_2CH_2CH_2CH_2CO$ of sebacate, $COCH_2CH_3$ of propionate, and $COCH_3$ of acetate), 3.00–5.20 (cellulose backbone), 5.11 ($CH_2C_6H_5$), 7.35 ($CH_2C_6H_5$).

Benzyl CAP suberate yield. 78.4% (2.79 mmol, 0.97 g). ^{1}H NMR ($CDCl_3$): 0.95–1.22 ($COCH_2CH_3$ of propionate), 1.33 ($COCH_2CH_2CH_2CH_2CH_2CH_2CO$ of suberate), 1.63 ($COCH_2CH_2CH_2CH_2CH_2CH_2CO$ of suberate), 2.10–2.46 ($COCH_2CH_2CH_2CH_2CH_2CH_2CO$ of suberate, $COCH_2CH_3$ of propionate, and $COCH_3$ of acetate), 3.00–5.20 (cellulose backbone), 5.10 (s, $CH_2C_6H_5$), 7.35 ($CH_2C_6H_5$).

A similar procedure was followed for the reaction of cellulose acetate butyrate (CAB-553-0.4, 1.00 g, 3.26 mmol) with monobenzyl suberoyl/sebacoyl chloride (1 equiv.).

Preparation of benzyl cellulose acetate suberate/sebacate. CA 320S (1.00 g, 4.19 mmol) was dissolved in DMI (20 mL), and the solution heated to 90 °C with stirring under N_2. Triethylamine (1.29 mL, 9.22 mmol, 2.2 equiv.) was added; a condenser was used to avoid evaporative loss of the base catalyst. Monobenzyl sebacoyl chloride (2.61 g, 8.38 mmol, 2 equiv.) or monobenzyl suberoyl chloride (2.41 g, 8.38 mmol, 2 equiv.) was added dropwise and allowed to react at 90 °C for 20 h. The reaction mixture was then filtered, and the remaining solution was diluted with ∼10 mL of acetone. The solution was precipitated in 300 mL of water. The precipitate was then collected and washed with isopropanol. The filtered product was redissolved in a minimal amount of THF and reprecipitated in hexanes.

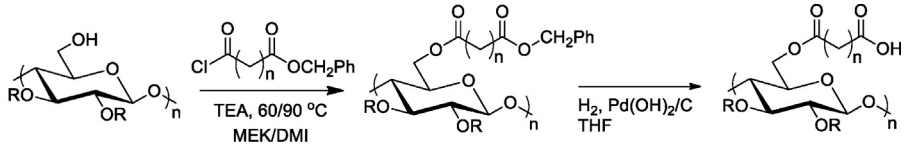

R: H or $COCH_3$ or $COCH_2CH_3$ or $COCH_2CH_2CH_3$. Note that the ester groups are randomly distributed at O-2,3,6, the particular positions of substitution are shown in Scheme 1 only for convenience of depiction

Scheme 1. General two-step synthetic method for ω-carboxyalkanoate derivatives of cellulose.

Reaction of cellulose in DMAc/LiCl solution with monobenzyl sebacoyl chloride. Microcrystalline cellulose (1.00 g, 6.17 mmol) was dissolved in DMAc (37.5 mL) and LiCl (1.88 g) by a procedure reported earlier (Edgar, Arnold, Blount, Lawniczak, & Lowman, 1995). The clear solution was heated to 60 °C and triethylamine (1.1 equiv. or 4 equiv.) was added. Monobenzyl suberoyl chloride (1 equiv. or 3 equiv.) was added dropwise and allowed to react for 20 h. For 1 equiv. reaction, the mixture was precipitated in 300 mL of DI water with slow addition, filtered, and the precipitate washed twice with 50 °C ethanol, then vacuum-dried. Yield: 78.6% (4.85 mmol, 1.52 g). For the 3 equiv. reaction, after precipitating in DI water, the aggregated product was ground using a mortar and pestle, Soxhlet-extracted with methanol overnight, and vacuum-dried. Yield: 94.8% (5.85 mmol, 4.09 g). Structural analysis by ^{1}H NMR was performed after peracylation.

A similar procedure was followed to synthesize benzyl cellulose suberate.

Peracylation. Benzyl cellulose suberate or sebacate (300 mg) was dissolved in 6 mL of pyridine, 25 mg 4-dimethylaminopyridine, and 5 mL of acetic or propionic anhydride. After stirring for 24 h at 80 °C, the product was precipitated into 250 mL water, collected by filtration, and then washed several times with water. The crude product was re-dissolved in 15 mL of CH_2Cl_2. This solution was added slowly with rapid stirring to 250 mL of ethanol. After filtration and washing with excess ethanol several times, the sample was dried under vacuum at 40 °C. ^{1}H NMR of peracetylated benzyl cellulose sebacate ($CDCl_3$): 0.94–1.35 ($COCH_2CH_2CH_2CH_2CH_2CH_2CH_2CO$ of sebacate), 1.50–1.72 ($COCH_2CH_2CH_2CH_2CH_2CH_2CH_2CO$ of sebacate), 1.82–2.25 ($COCH_3$ of acetate), 2.32 ($COCH_2CH_2CH_2CH_2CH_2CH_2CH_2CO$ of sebacate), 3.00–5.20 (cellulose backbone), 5.11 ($CH_2C_6H_5$), 7.33 ($CH_2C_6H_5$).

Pd(OH)$_2$/C hydrogenolysis of the benzyl cellulose ester (Scheme 1). To a solution of 500 mg benzyl cellulose mixed ester dissolved in 50 mL of anhydrous THF, 500 mg palladium hydroxide, 20 wt% Pd (dry basis) on carbon was added. A hydrogen balloon was attached to the flask, and the solution stirred overnight under H_2 at room temperature. The mixture was filtered through Celite and concentrated. The product was dissolved in dichloromethane and precipitated into hexanes. The precipitate was collected and dried under vacuum. For benzyl CA 320S suberate and sebacate esters, a second hydrogenolysis reaction was required to achieve complete cleavage of the benzyl ester bond.

CAP sebacate yield. 96.1% (1.39 mmol, 0.45 g). ^{1}H NMR (d_6-DMSO): 0.80–1.10 ($COCH_2CH_3$ of propionate), 1.22 ($COCH_2CH_2CH_2CH_2CH_2CH_2CH_2CO$ of sebacate), 1.45 ($COCH_2CH_2CH_2CH_2CH_2CH_2CH_2CH_2CO$ of sebacate), 2.05–2.52 ($COCH_2CH_2CH_2CH_2CH_2CH_2CH_2CH_2CO$ of sebacate, $COCH_2CH_3$ of propionate, and $COCH_3$ of acetate), 2.80–5.30 (cellulose backbone).

Preparation of amorphous solid dispersions by co-precipitation. Powder solid dispersion systems of 1/3 (w/w) ritonavir/cellulose ω-carboxyalkanoate (50 mg/150 mg) were prepared as follows: accurately weighed quantities of polymer and drug were dissolved in 32 mL acetone (or THF if the polymer was not soluble in acetone), then the homogeneous solution was added into 150 mL water with vigorous stirring. The organic solvent was removed under reduced pressure by rotary evaporation at 40 °C. The aqueous drug/polymer mixture was freeze-dried at −53 °C for 2 days to obtain solid powder.

Solubility parameter (SP) of cellulose ω-carboxyalkanoates. SP calculations were used to compare the relative hydrophobicities of the polymers. SP values were estimated using the method proposed by Fedors (1974). The method is based on group additive constants and the contribution of a large number of functional groups was evaluated, therefore this method requires only knowledge of the structural formula of the polymer. Solubility parameter can be evaluated using:

$$\delta = \sqrt{\frac{\sum_i \Delta e_i}{\sum_i \Delta v_i}} = \sqrt{\frac{\Delta E_v}{V}} \quad (1)$$

where Δe_i and Δv_i are the additive atomic and group contribution for the energy of vaporization and molar volume, respectively. The contributions applicable at a temperature of 25 °C are presented in the reference (Fedors, 1974). For high molecular weight polymers that have $T_g > 25$ °C, there is a deviation between the experimentally measured ΔE_v and V and the estimated values. A small correction factor was introduced to take into account the divergence in the V values:

$$\Delta v_i = 4n, \quad n < 3 \quad (2)$$

$$\Delta v_i = 2n, \quad n \geq 3 \quad (3)$$

where n is the number of main chain skeletal atoms in the smallest repeating unit of the polymer.

Crystal growth rate of ritonavir. Crystal growth rate was characterized by measuring the rate of desupersaturation in the presence of seed crystals. Crystal growth rate experiments were performed in the presence and absence of pre-dissolved cellulose derivatives and the initial ritonavir concentration was 10 μg/mL. Polymer concentrations of 5 μg/mL were used and all experiments were performed in triplicate. The solubility of crystalline ritonavir is known not to change in 5 μg/mL polymer solutions. The rate of desupersaturation of ritonavir was measured using an SI Photonics (Tuscon, AZ) UV spectrometer coupled to a fiber optic probe (path-length 5 mm) at a constant temperature of 37 °C. Data were acquired at 5 s time intervals within wavelengths ranging from 200 to 450 nm. The ritonavir peak was detected at 240 nm. Supersaturated solutions were generated by adding a small volume of pre-dissolved ritonavir in methanol to 100 mM sodium phosphate buffer, pH 6.8. Prior to addition of solubilized ritonavir, seed crystals were added to the buffer and allowed to equilibrate at 37 °C. Data collection began immediately after generation of supersaturation. An overhead stirrer was used to stir the solution at a speed of 400 rpm. The slope of the concentration vs. time curve over the first 2 min of the experiment was taken as the initial crystal growth rate. In order to mitigate particle scattering effects, second derivatives (SIMCA P+ V. 12 software (Umetrics Inc., Umea, Sweden) of the spectra were taken for the sample data.

3. Results and discussion

3.1. Synthesis and characterization of cellulose ω-carboxyalkanoates

In our previous work on synthesis of cellulose ester adipates, we found that reaction of cellulose esters with adipic anhydride could lead to crosslinked, insoluble products because of reaction of multiple cellulose chains with poly(adipic anhydride) contaminant in the adipic anhydride (Kar et al., 2011). Though we later developed a carefully designed procedure that circumvented these issues and permitted use of adipic anhydride reagent to afford soluble cellulose ester adipates (Liu et al., 2012), we found in the interim that there was a more forgiving, if slightly less direct approach. We found that conversion of adipic acid into a mono-functional, mono-protected reagent provided a useful route for synthesis of cellulose ester adipates for our initial structure–property studies. Fischer esterification of the diacid with benzyl alcohol afforded a mixture of diester, monoester, and starting diacid, from which the monoester could be readily isolated in reasonable yield; this was then smoothly converted using oxalyl chloride/DMF to the

monoacid chloride. Commercially available cellulose esters were reacted with the product monobenzyl adipoyl chloride to generate protected cellulose ester adipates. Finally, mild hydrogenation removed the benzyl protective group to afford the cellulose adipate esters.

We planned to follow a similar approach for the synthesis of cellulose ester suberates and sebacates (suberic and sebacic anhydrides would have large and unfavorable (9 and 11 membered, respectively) ring sizes and to our knowledge are unknown). We were however cognizant that the synthesis of the monoprotected, monofunctional reagents required could be more complicated due to solubility issues, and that often reaction of longer chain reagents with cellulose can be difficult (Edgar, 2009). Indeed, we found that using the same methodology we employed for monobenzyl adipate synthesis gave exceptionally low yields of monobenzyl suberate and monobenzyl sebacate. We investigated stoichiometric as well as work up issues to improve the yields. In the monobenzyl adipate synthesis, a molar ratio of benzyl alcohol to di-acid of 1.5 was most effective, in spite of the excess benzyl alcohol that might be expected to generate an excessive amount of dibenzyl adipate. We were also concerned that the strongly basic conditions (NaOH) used in the adipate workup might be reducing yield due to ester hydrolysis. We reduced the molar ratio of benzyl alcohol to diacid to 1.2, to minimize generation of the dibenzyl suberate or sebacate. By extracting residual diacid with aqueous 1 M $NaHCO_3$, we were able to avoid excessive hydrolysis (NaOH) or poor separation of layers (Na_2CO_3), while still ensuring quantitative removal of diacid (crucial since residual diacid would be converted to a diacid chloride in the ensuing step, leading to polymer crosslinking). ^{1}H NMR confirmed that the product monobenzyl esters, obtained in moderate yields, were pure and uncontaminated by dibenzyl esters or unreacted diacid.

Subsequent conversion of monobenzyl suberate and monobenzyl sebacate to the corresponding monoacid chlorides went very smoothly using oxalyl chloride/DMF, affording more than 90% yield in each case of crude products that were not purified, but were shown by ^{1}H NMR to have the desired monoprotected, monofunctional structures (Supplementary materials, Figs. S3 and S4). Both products were reactive yellow liquids that were stable if stored at 4 °C.

Reactions of these monofunctional reagents with commercially available cellulose esters in common organic solvents were facile, with no sign of crosslinking. Three different commercially available cellulose esters, cellulose acetate propionate (CAP-504-0.2), cellulose acetate butyrate (CAB-553-0.4) and cellulose acetate (CA 320S), were selected due to their solvent solubility and high number of hydroxyls available for reaction (see Table 1 for details on substituent DS); this also gave us a range of hydrophobicity that would facilitate our structure–property studies. CAP-504-0.2 and CAB-553-0.4 were reacted with the acid chlorides in methyl ethyl ketone (MEK). The low DS CA we used is insoluble in MEK, so instead was dissolved in warm 1,3-dimethyl-2-imidazolidinone (DMI). MEK is preferred over acetone due to its higher boiling point, permitting the reaction to be run under more energetic conditions (60 °C). The nature of this condensation reaction is such that there should be considerable flexibility with regard to reaction solvent.

Substituent DS values in these protected cellulose sebacate/suberate products were calculated by integrating the cellulose backbone and benzylic hydrogen peaks together and calculating the ratio to the phenyl protons (Fig. 1; sample calculation Appendix 1). As shown in Table 1, sebacate DS in cellulose acetate propionate sebacate (CAP Seb) responded in straightforward fashion to an increase in monobenzyl sebacoyl chloride (BnSeCl) used, affording nearly 3-fold increase in DS (Seb) with a three-fold increase in acid chloride. We observe that ω-carboxyalkanoyl DS values decrease slightly for the CAB and CAP polymers as the diacid chain gets longer. This can be rationalized by steric hindrance. Similarly, CAP derivatives consistently have higher ω-carboxyalkanoyl DS values than the corresponding CAB derivatives, with the obvious culprit being poorer accessibility of the OH groups on cellulose in the presence of the longer butyrate chains. CA 320S has less bulky substituents and higher hydroxyl content, thus by using 2 equiv. monobenzyl sebacoyl chloride per CA 320S AGU, the DS of benzyl-protected carboxyester can be up to 0.57. All these benzyl-protected intermediate products are quite soluble in organic solvents, for example in THF.

Hydrogenolysis of the benzyl ester groups on protected cellulose adipates, for example on protected CAAdP, can be slightly sluggish, occasionally requiring longer reaction times or re-hydrogenation. In contrast, the longer and more flexible suberate and sebacate chains are more suitable for heterogeneous catalytic hydrogenation, so that all benzyl cellulose suberate and sebacate hydrogenation reactions were facile and straightforward, achieving clean hydrogenolysis of the benzyl ester. Use of $Pd(OH)_2/C$ catalyst enables reaction completion overnight at room temperature on the gram scale. Both ^{1}H NMR and ^{13}C NMR spectra (Fig. 2a and b) show the disappearance of benzylic and aromatic signals, without any observable residual substitution. In larger scale reactions it may be necessary to perform the hydrogenation reaction twice to obtain complete hydrogenolysis.

It was important to determine the relationship between cellulose ω-carboxyalkanoate structure and thermal properties. T_g in particular is important in ASDs; the high T_g values for most known cellulose esters are advantageous in ASD formulations, since they ensure that the formulation T_g will remain well above ambient temperature even when containing a substantial portion of drug (which may be a plasticizer) and at high ambient humidity (water will definitely be a plasticizer). Keeping the formulation T_g well above ambient temperature ensures that the matrix is in the glassy state, preventing drug migration through the matrix that could lead to crystallization (Shelton et al., 2009). From the thermogram we are also able to observe whether the polymer itself has a tendency to crystallize. Thermal properties of cellulose suberate and sebacate mixed esters after deprotection are summarized in Table 1.

Table 1
Cellulose suberate/sebacate mixed-esters syntheses, DS values, and properties.

Sample	Starting CE	Carboxy-ester	Solvent	Temp (°C)	Molar ratio[a]	DS (COOH)	DS (Other)	DS (Total)	T_g (°C)	M_n (g/mol)	DP
1	CAP-504-0.2	Sub	MEK	60	1	0.27	Pr 2.09 Ac 0.04	2.39	120	16.7	52
2	CAP-504-0.2	Seb	MEK	60	1	0.24	Pr 2.09 Ac 0.04	2.37	116	18.8	58
3	CAP-504-0.2	Seb	MEK	60	3	0.67	Pr 2.09 Ac 0.04	2.80	78	19.1	47
4	CAB-553-0.4	Sub	MEK	60	1	0.26	Bu 1.99 Ac 0.14	2.39	89	20.9	60
5	CAB-553-0.4	Seb	MEK	60	1	0.22	Bu 1.99 Ac 0.14	2.37	89	22.6	65
6	CA 320S	Sub	DMI	90	2	0.63	Ac 1.82	2.45	101	21.2	63
7	CA 320S	Seb	DMI	90	2	0.57	Ac 1.82	2.39	117	25.0	73

Abbreviations. Sub, suberate; Seb, sebacate; Ac, acetate; Pr, propionate; Bu, butyrate.

[a] Mol monobenzyl acid chloride per mol anhydroglucose unit.

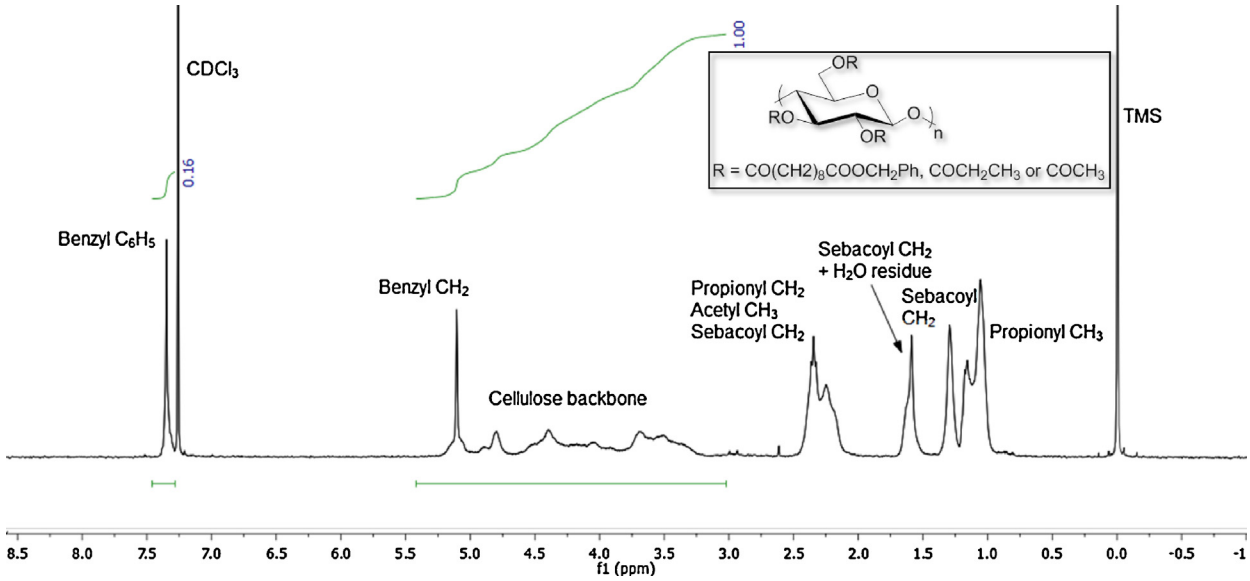

Fig. 1. ^{1}H NMR of benzyl CAP-504-0.2 sebacate (DS Se = 0.24) in $CDCl_3$.

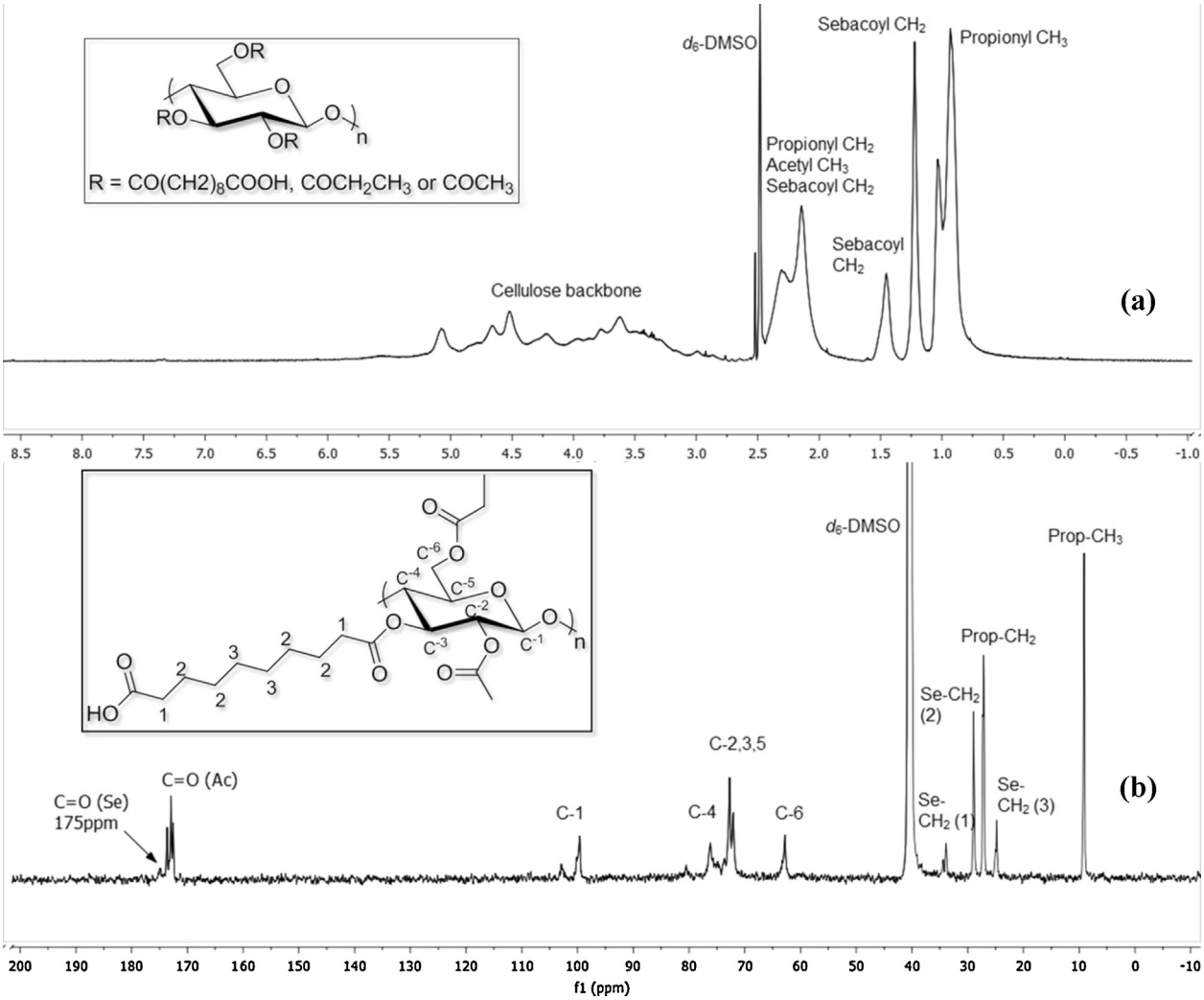

Fig. 2. ^{1}H NMR (a) and ^{13}C NMR (b) of CAP-504-0.2 sebacate (DS Se = 0.24) in d_6-DMSO.

T_g values of the products are generally 40–80 °C lower than the starting cellulose esters due to the plasticizing effect of the polymethylene chains of the pendent ω-carboxyalkanoyl groups. DSC results also showed that T_g depression increased with increasing chain length and increasing DS. Even so, T_g values of these deprotected cellulose ω-carboxyalkanoates are at least 50 °C higher than the highest anticipated ambient temperatures, indicating adequacy for ASDs. Degree of polymerization (DP) data for CAP and CAB derivatives indicate that little or no cellulose chain degradation occurred during acylation and deprotection, consistent with the relatively mild conditions applied. It should be noted that the DP of CAP Seb (DS Se = 0.24) slightly exceeds the DP of the starting CAP (Supplementary material, Table S1); it is reasonable to speculate that the carboxyl-containing cellulosic polymers can self-aggregate in THF solvent (Kar et al., 2011). For CA derivatives, the DPs are reduced to less than half that of the starting CA-320S, presumably due to the higher reaction temperatures employed (90 °C) in acylation of CA.

3.2. Regioselectivity

It was of interest to explore the regioselectivity of reaction of cellulose with the monoprotected long chain diacid chlorides, since substitution regioselectivity has been shown to have powerful influence on properties like solubility, thermal properties, and optical properties (Tasaka et al., 2006) to name just a few such relationships (Fox, Li, Xu, & Edgar, 2011). To investigate regioselectivity, microcrystalline cellulose was reacted in DMAc/LiCl solution with monobenzyl suberoyl/sebacoyl chlorides. The benzyl cellulose suberate and sebacate products from acylation in DMAc/LiCl are only sparingly soluble in DMSO. To obtain a well-resolved NMR spectrum, peracetylation was performed to provide products that were readily soluble in chloroform. DS (ω-carboxyester) was calculated based on the ratio of the integrals of benzyl ring protons to those of the benzyl methylene and the cellulose backbone overlapping from 3.00 to 5.20 ppm. At a ratio of 1 equiv. BnSeCl per AGU, a DS of 0.55 was obtained with a reaction time of 20 h at 60 °C. Using 3 equiv. BnSeCl per AGU under the same conditions, a higher DS (1.95) was achieved. Benzyl cellulose sebacate with high ω-carboxyester substitution tends to self-aggregate in water, therefore grinding and extra washing steps are necessary to remove the impurities before peracetylation.

As predicted from our previous study with very bulky acid chlorides like pivaloyl chloride (Xu, Li, Tate, & Edgar, 2011), regioselectivity was quite limited. After peracetylation of benzyl cellulose sebacate (DS Seb = 1.95), acetyl methyls at O-6 (2.10 ppm), O-2 (1.97 ppm) and O-3 (1.90 ppm) could still be observed by ^{1}H NMR (Supplementary material, Fig. S14). Table S2 (Supplementary material) summarizes the total/partial DS values according to corresponding reaction feed ratio and substitution type.

The ^{13}C NMR spectrum of peracetylated cellulose sebacate (DS Seb = 0.55) further confirmed the lack of regioselectivity of this reaction (Fig. 3). The hydrogenated product is readily soluble in DMSO. Acetyl carbonyl carbons at 170.0, 169.1 and 168.8 ppm were correlated in heteronuclear multibond correlation spectroscopy (HMBC) with AGU protons at the sites of acetylation at O-6, O-3 and O-2, respectively (Iwata, Azuma, Okamura, Muramoto, & Chun, 1992). HMBC is not sensitive enough to provide the exact distribution of sebacate group with much lower substitution, but fortunately, the sebacoyl carbonyl carbons demonstrate as well three different peaks near downfield around 171–174 ppm.

3.3. Effect of newly synthesized polymers on solution crystal growth inhibition of ritonavir

Supersaturating dosage forms, such as amorphous solids, are attractive for improving the delivery of poorly water soluble drugs since they result in a solution with a higher thermodynamic activity which may enhance the absorption of a drug relative to a saturated solution (Warren, Benameur, Porter, & Pouton, 2010). However, in order to maintain supersaturation, crystallization must be prevented and hence the presence of an effective crystal growth inhibitor in solution is desirable to prolong supersaturation. While polymers are often used to fulfill this role (Alonzo et al., 2012; Lechuga-Ballesteros & Rodriguez-Hornedo, 1995a; Lechuga-Ballesteros & Rodriguez-Hornedo, 1995b; Zimmermann et al., 2009), there is little mechanistic understanding of the properties of a polymer that make it a good inhibitor of crystal growth for a given compound. In a previous study (Ilevbare et al., 2012b), the effectiveness of a group of chemically diverse polymers, including a number of novel cellulose ω-carboxyalkanoates, at inhibiting the crystal growth of ritonavir from solution was quantified. It was found that moderately hydrophobic polymers were more effective crystal growth inhibitors of the hydrophobic drug, ritonavir, than

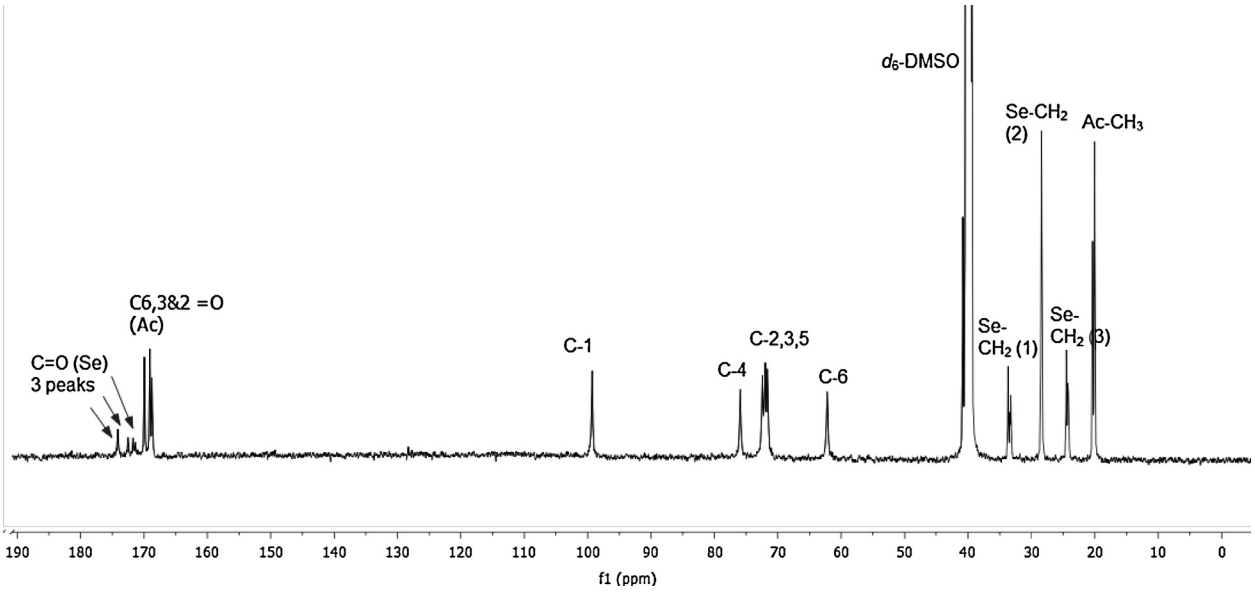

Fig. 3. ^{13}C NMR of fully-substituted cellulose acetate sebacate (DS Se = 0.55) in d_6-DMSO.

Table 2
DS and SP values for cellulose derivatives and their ranking.

Polymer abbreviation	DS (CO_2H)	DS (Other)	DS (Total)	DS (CO_2H) Rank	SP ($MPa^{1/2}$)	SP Rank
CP Adp	0.48	Pr 1.68	2.16	6	23.28	1
CA 320S Adp	0.67	Ac 1.82	2.49	3	22.95	2
CA 320S Sub	0.63	Ac 1.82	2.45	4	22.62	3
CA 320S Seb	0.57	Ac 1.82	2.39	5	22.36	4
CAP Adp 0.85	0.85	Ac 0.04; Pr 2.09	2.98	1	21.27	5
CAB Adp 0.81	0.81	Ac 0.14; Bu 1.99	2.84	2	20.86	6
CAP Adp 0.33	0.33	Ac 0.04; Pr 2.09	2.46	7	20.56	7
CAP Seb 0.67	0.67	Ac 0.04; Pr 2.09	2.80	3	20.41	8
CAP Sub	0.27	Ac 0.04; Pr 2.09	2.39	8	20.19	9
CAB Adp 0.25	0.25	Ac 0.14; Bu 1.99	2.38	10	20.05	10
CAP Seb 0.24	0.24	Ac 0.04; Pr 2.09	2.37	11	19.94	11
CAB Sub	0.26	Ac 0.14; Bu 1.99	2.38	9	19.84	12
CAB Seb	0.22	Ac 0.14; Bu 1.99	2.35	12	19.62	13

Abbreviations: Ac, acetate; Pr, propionate; Bu, butyrate; Adp, adipate; Sub, suberate; Seb, sebacate.

either highly hydrophilic or highly hydrophobic polymers. In addition, the novel cellulose-based polymers containing a higher DS of ionizable carboxylic acids were better inhibitors relative to less ionized cellulose polymers. We have evaluated the effectiveness of several of the newly synthesized cellulose ω-carboxyalkanoates in inhibiting crystal growth of ritonavir from supersaturated solution, in comparison with that of previously synthesized and reported cellulose derivatives (Kar et al., 2011). Ritonavir was chosen as the model compound due to its very low aqueous solubility. Aqueous insolubility results primarily from high log *P* (lipophilicity) and/or high melting point, T_m (representing lattice energy). Ritonavir is a highly lipophilic compound with a log *P* value of 5.98 and melting point of 121 °C (Baird, Van Eerdenbrugh, & Taylor, 2010; Murdande, Pikal, Shanker, & Bogner, 2010), yielding an equilibrium solubility of 1.3 ± 0.10 μg/mL, at pH 6.8 (ritonavir is un-ionized at this pH) and 37 °C.

Ritonavir crystal growth rate in the absence and presence of the novel cellulosic polymers was determined using the method previously described (Ilevbare et al., 2012b). The novel cellulose derivatives used in this report and some of their properties are presented in Table 2. Solubility parameters (SP), estimated according to the method of Fedors (1974), were used to rank relative polymer hydrophobicity. The solubility parameter provides a numerical estimate of the intermolecular forces within a material, and can be a good indication of solubility, particularly for non-polar materials such as polymers. The hydrophobicity ranking is presented, where the least hydrophobic polymer, CP Adp is ranked #1 and #13 represents the most hydrophobic polymer, CAB Seb. The DS values of carboxyl-containing substituents (DS (CO_2H)) of the new cellulose esters are also listed and ranked in Table 2.

Fig. 4 compares the growth rate ratio of ritonavir (10 μg/mL, S of 7.6) in the absence of polymer (R_{g0}) to that in the presence of polymer (R_{gp}). Polymers are arranged in order of increasing hydrophobicity (*L* to *R*). Polymers with an effectiveness ratio greater than 1 ($R_{g0}/R_{gp} > 1$) are considered effective crystal growth inhibitors. With the exception of the data for the CA 320S sebacates and suberates, we have previously reported effectiveness ratios for the other cellulose ω-carboxyalkanoates. Out of the 13 cellulose ω-carboxyalkanoates presented in Fig. 4, 6 were ineffective, while 7 were effective at inhibiting crystal growth, albeit to varying extents. Polymers located in the middle portion of Fig. 4 (i.e. moderately hydrophobic polymers (20.56–22.62 $MPa^{1/2}$)) were the most effective crystal growth inhibitors. In the previous study, CAP Adp 0.85 and CAB Adp 0.81 were identified as the most effective cellulose-based polymers (Ilevbare et al., 2012b). However, two of the new cellulose ω-carboxyalkanoate polymers, CA320S Sub and CA320S Seb, were significantly more effective at inhibiting the crystal growth of ritonavir. Together with the relatively high DS of the suberate and sebacate substituents (more ionizable carboxylic acids), combining the relatively more hydrophilic cellulose ester (CA320S) with the longer chain ω-carboxyalkanoate (e.g. suberate and sebacate) resulted in polymers with an optimal level of hydrophobicity, thus making CA320 Sub and CA320 Seb very effective crystal growth inhibitors. This further supports the importance of hydrophobicity as a key factor influencing polymer effectiveness.

3.4. ASDs of ritonavir in cellulose ω-carboxyalkanoate matrices

We prepared ASDs of the model drug ritonavir in cellulose ω-carboxyalkanoates by co-precipitation of a solution of drug and polymer in a common solvent (acetone or THF) into a common non-solvent, water, followed by solvent removal by rotary evaporation and lyophilization to remove water. Spray drying was not practical due to the small amounts of each novel polymer available. ASD samples were characterized by PXRD to determine the

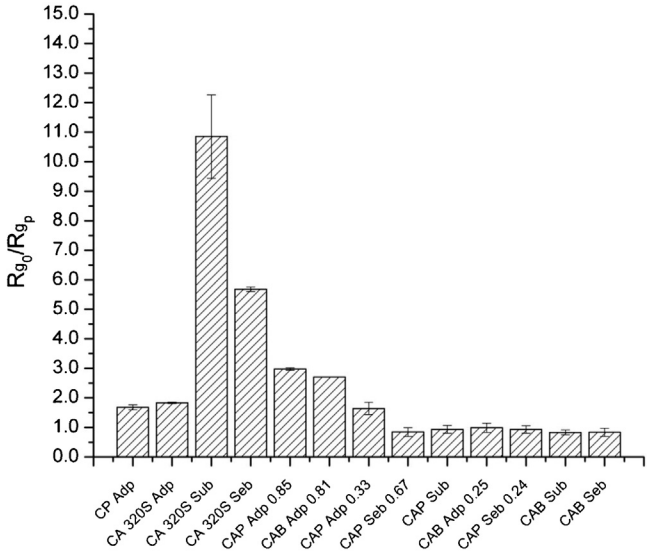

Fig. 4. Crystal growth rate ratio of ritonavir at an initial ritonavir concentration of 10 μg/mL. The data is arranged in order of hydrophobicity: least hydrophobic to most hydrophobic (left to right). Crystal growth rate experiments were performed in triplicate. Each column is an average of the effectiveness ratio and error bars indicate one standard deviation. The *y*-axis is a ratio of the growth rate of ritonavir in the absence of polymer to growth rate of ritonair in the presence of polymer (5 μg/mL). Polymers with a ratio > 1 are considered effective crystal growth inhibitors. With the exception of CA 320S Sub and CA 320S Seb, the effectiveness growth ratios for all cellulose ω-carboxyalkanoates were previously reported (Ilevbare et al., 2012b).

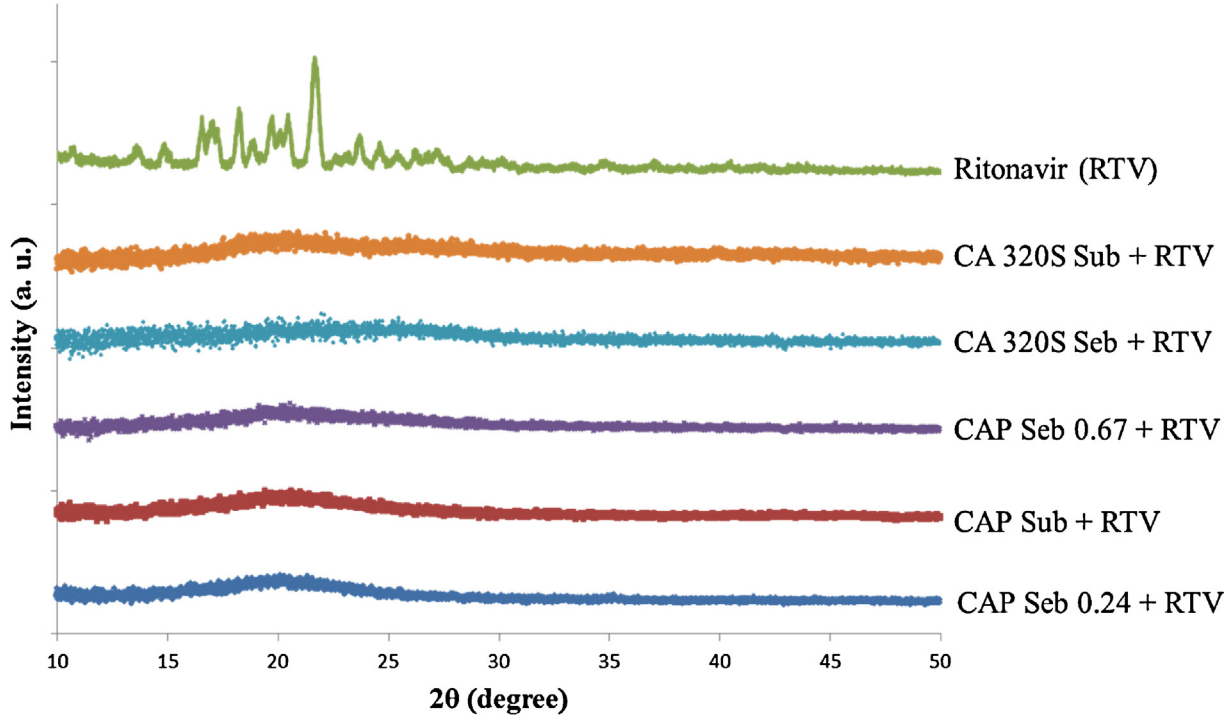

Fig. 5. PXRD pattern of ritonavir crystalline powder and amorphous solid dispersions prepared by co-precipitation with cellulose ω-carboxyalkanoates.

crystallinity of the ritonavir in the ASD (Fig. 5). PXRD patterns of all polymer/RTV 3/1 ASD were devoid of the diffraction peaks evident in the XRD pattern of crystalline ritonavir, indicating that ritonavir is completely amorphous in these blends. To further confirm their amorphous nature, DSC thermograms (Fig. S17, Supplementary material) of the ASDs showed single, broad glass transitions, whereas the melting endotherm of crystalline ritonavir at ~125 °C was not observed. Based on our previous work and that of others, we expect that the aqueous solution concentrations of ritonavir released from these ASDs will be significantly increased vs. that from crystalline drug. Determination of solubility enhancement (supersaturation) versus time and other drug release studies will be discussed in a forthcoming paper.

4. Conclusions

Successful pathways were developed for the synthesis of cellulose ω-carboxyalkanoates by reaction of cellulose, CAP, CAB and CA with monobenzyl suberoyl and monobenzyl sebacoyl chlorides. Barriers to acid chloride synthesis were overcome to develop reasonably efficient processes. Condensation of acid chlorides with cellulose esters can be carried out in common organic solvents under mild conditions, and appears to be capable of affording a wide range of DS ω-carboxyalkanoates. Even though a relatively bulky benzyl-protected long chain diacid was incorporated, virtually no regioselectivity of substitution was observed. Debenzylation of these long chain benzyl cellulose ω-carboxyalkanoates was facile under mild conditions in the presence of a palladium catalyst. The resulting carboxyl-containing mixed esters are well suited as ASD polymers for oral drug delivery, and most of them form amorphous dispersions with the hydrophobic drug ritonavir. All of them possess T_g values adequate to prevent drug recrystallization in the solid phase. Most importantly, CA 320S suberate and sebacate are at least 5-fold more effective as inhibitors of ritonavir crystallization from aqueous solution than other cellulosic and non-cellulosic ASD polymers. We will further explore these novel cellulose ω-carboxyalkanoates with respect to the degree and duration of solution concentration enhancement, its generality with respect to drug structure, and the mechanism of solubilization in forthcoming reports.

Acknowledgments

This project was supported primarily by a grant from the National Science Foundation (NSF, grant number DMR-0804501). We thank Eastman Chemical Company for their kind donation of the commercial cellulose esters used in this work, and the Macromolecules and Interfaces Institute and the Institute for Critical Technologies and Applied Science at Virginia Tech for their financial, facilities, and educational support. We also thank Alison Shultz for SEC analyses, Rick Caudill for XRD experiments and Bruce Orler for some of the DSC measurements (all from Virginia Tech).

Appendix A. Appendix 1. The degree of substitution (DS) values were determined according to the following equation

$$\text{DS } \omega\text{-carboxyester} = \frac{7I_{\text{phenyl}}}{5I_{\text{backbone+benzylic hydrogen}} - 2I_{\text{phenyl}}}$$

Appendix B. Supplementary data

Supplementary data associated with this article can be found, in the online version, at http://dx.doi.org/10.1016/j.carbpol.2012.11.049.

References

Abell, A. D., Morris, K. B., & Litten, J. C. (1990). Synthesis and deprotection of [1-(ethoxycarbonyl)-4-[(diphenylmethoxy)carbonyl]-1-methyl-2-oxobutyl]triphenylphosphonium chloride: A key intermediate in the Wittig reaction between a cyclic anhydride and a stabilized ylide. *Journal of Organic Chemistry*, *55*, 5217–5221.

Alonzo, D. E., Gao, Y., Zhou, D., Mo, H., Zhang, G. G. Z., & Taylor, L. S. (2011). Dissolution and precipitation behavior of amorphous solid dispersions. *Journal of Pharmaceutical Sciences*, *100*, 3316–3331.

Alonzo, D. E., Raina, S., Zhou, D., Gao, Y., Zhang, G. G. Z., & Taylor, L. S. (2012). Characterizing the impact of hydroxypropylmethyl cellulose on the growth and nucleation kinetics of felodipine from supersaturated solutions. *Crystal Growth and Design*, *12*, 1538–1547.

Alonzo, D. E., Zhang, G. G., Zhou, D., Gao, Y., & Taylor, L. S. (2010). Understanding the behavior of amorphous pharmaceutical systems during dissolution. *Pharmaceutical Research*, *27*, 608–618.

Baird, J. A., Van Eerdenbrugh, B., & Taylor, L. S. (2010). A classification system to assess the crystallization tendency of organic molecules from undercooled melts. *Journal of Pharmaceutical Sciences*, *99*, 3787–3806.

Cameron, W., Japour, A. J., Xu, Y., Hsu, A., Mellors, J., Farthing, C., et al. (1999). Ritonavir and saquinavir combination therapy for the treatment of HIV infection. *AIDS*, *13*, 213–224.

Edgar, K. J. (2009). Direct synthesis of partially substituted cellulose esters. In K. J. Edgar, C. M. Buchanan, & T. Heinze (Eds.), *Polysaccharide materials: Performance by design* (pp. 213–229). Washington, DC: American Chemical Society.

Edgar, K. J., Arnold, K. M., Blount, W. W., Lawniczak, J. E., & Lowman, D. W. (1995). Synthesis and properties of cellulose acetoacetates. *Macromolecules*, *28*, 4122–4128.

Edgar, K. J., Buchanan, C. M., Debenham, J. S., Rundquist, P. A., Seiler, B. D., Shelton, M. C., et al. (2001). Advances in cellulose ester performance and application. *Progress in Polymer Science*, *26*, 1605–1688.

English, A. R., Girard, D., Jasys, V. J., Martingano, R. J., & Kellogg, M. S. (1990). Orally effective prodrugs of the beta-lactamase inhibitor sulbactam. *Journal of Medicinal Chemistry*, *33*, 344–347.

Fedors, R. F. (1974). Method for estimating both the solubility parameters and molar volumes of liquids. *Polymer Engineering and Science*, *14*, 147–154.

Fox, S. C., Li, B., Xu, D., & Edgar, K. J. (2011). Regioselective esterification and etherification of cellulose: A review. *Biomacromolecules*, *12*, 1956–1972.

Friesen, D. T., Shanker, R., Crew, M., Smithey, D. T., Curatolo, W. J., & Nightingale, J. A. (2008). Hydroxypropyl methylcellulose acetate succinate-based spray-dried dispersions: An overview. *Molecular Pharmacology*, *5*, 1003–1019.

Hancock, B. C., Shamblin, S. L., & Zografi, G. (1995). Molecular mobility of amorphous pharmaceutical solids below their glass transition temperatures. *Pharmaceutical Research*, *12*, 799–806.

Hauss, D. J. (2007). Oral lipid-based formulations. *Advanced Drug Delivery Reviews*, *59*, 667–676.

Ilevbare, G., Liu, H., Edgar, K. J., & Taylor, L. (2012). Inhibition of solution crystal growth of ritonavir by cellulose polymers—Factors influencing polymer effectiveness. *CrystEngComm*, *14*, 6503–6514.

Ilevbare, G. A., Liu, H., Edgar, K. J., & Taylor, L. S. (2012). Understanding polymer properties important for crystal growth inhibition—Impact of chemically diverse polymers on solution crystal growth of ritonavir. *Crystal Growth and Design*, *12*, 3133–3143.

Iwata, T., Azuma, J., Okamura, K., Muramoto, M., & Chun, B. (1992). Preparation and NMR assignments of cellulose mixed esters regioselectively substituted by acetyl and propanoyl groups. *Carbohydrate Research*, *224*, 277–283.

Kar, N., Liu, H., & Edgar, K. J. (2011). Synthesis of cellulose adipate derivatives. *Biomacromolecules*, *12*, 1106–1115.

Konno, H., Handa, T., Alonzo, D. E., & Taylor, L. S. (2008). Effect of polymer type on the dissolution profile of amorphous solid dispersions containing felodipine. *European Journal of Pharmaceutics and Biopharmaceutics*, *70*, 493–499.

Lechuga-Ballesteros, D., & Rodriguez-Hornedo, N. (1995a). Effects of molecular structure and growth kinetics on the morphology of L-alanine crystals. *International Journal of Pharmaceutics*, *115*, 151–160.

Lechuga-Ballesteros, D., & Rodriguez-Hornedo, N. (1995b). The influence of additives on the growth kinetics and mechanism of L-alanine crystals. *International Journal of Pharmaceutics*, *115*, 139–149.

Li, B., Konecke, S., Wegiel, L., Taylor, L. S., & Edgar, K. J. (2012). Both solubility and chemical stability of curcumin are enhanced by solid dispersion in cellulose derivative matrices, under review.

Liu, H., Kar, N., & Edgar, K. J. (2012). Direct synthesis of cellulose adipate derivatives using adipic anhydride. *Cellulose*, *19*, 1279–1293.

Mawad, D., Mouaziz, H., Penciu, A., Méhier, H., Fenet, B., Fessi, H., et al. (2009). Elaboration of radiopaque iodinated nanoparticles for in situ control of local drug delivery. *Biomaterials*, *30*, 5667–5674.

Murdande, S. B., Pikal, M. J., Shanker, R. M., & Bogner, R. H. (2010). Solubility advantage of amorphous pharmaceuticals: II. Application of quantitative thermodynamic relationships for prediction of solubility enhancement in structurally diverse insoluble pharmaceuticals. *Pharmaceutical Research*, *27*, 2704–2714.

Newman, A., Knipp, G., & Zografi, G. (2012). Assessing the performance of amorphous solid dispersions. *Journal of Pharmaceutical Sciences*, *101*, 1355–1377.

Posey-Dowty, J. D., Watterson, T. L., Wilson, A. K., Edgar, K. J., Shelton, M. C., & Lingerfelt, L. R., Jr. (2007). Zero-order release formulations using a novel cellulose ester. *Cellulose*, *14*, 73–83.

Shelton, M. C., Posey-Dowty, J. D., Lingerfelt, L. R., Kirk, S. K., Klein, S., & Edgar, K. J. (2009). Enhanced dissolution of poorly soluble drugs from solid dispersions in carboxymethylcellulose acetate butyrate matrices. In K. J. Edgar, T. Heinze, & T. Liebert (Eds.), *Polysaccharide materials: Performance by design* (pp. 93–113). Washington, DC: American Chemical Society.

Tasaka, K., Umeda, H., Kuzuhara, N., & Yajima, T. (2006). Cellulose ester film, manufacturing, optical retardation film, optical compensation sheet, elliptic polarizing plate, and image display. US Patent 7,038,744.

Warren, D. B., Benameur, H., Porter, C. J. H., & Pouton, C. W. (2010). Using polymeric precipitation inhibitors to improve the absorption of poorly water-soluble drugs: A mechanistic basis for utility. *Journal of Drug Targeting*, *18*, 704–731.

Xu, D., Li, B., Tate, C., & Edgar, K. J. (2011). Studies on regioselective acylation of cellulose with bulky acid chlorides. *Cellulose*, *18*, 405–419.

Zimmermann, A., Millqvist-Fureby, A., Elema, M. R., Hansen, T., Muellertz, A., & Hovgaard, L. (2009). Adsorption of pharmaceutical excipients onto microcrystals of siramesine hydrochloride: Effects on physicochemical properties. *European Journal of Pharmaceutics and Biopharmaceutics*, *71*, 109–116.